Adsorption of Nitrogen and Sulphur Organic-Compounds on Titania Nanotubes

A. Rendon-Rivera[1], M.A. Cortes-Jacome[2], E. López-Salinas[3], M.L. Mosqueira[4], J.A. Toledo-Antonio[5]*

Instituto Mexicano del Petróleo, Eje Central Lázaro Cárdenas # 152, San Bartolo Atepehuacan, G. A. Madero, 07730 México, D.F., México
*Corresponding Author e-mail: jtoledo@imp.mx

Abstract— *Anatase TiO_2 nanoparticles and TiO_2 nanotubes were used as adsorbents to determine their selective adsorption properties on liquid-phase pure S- or N-organic compounds (dibenzothiophene (DBT), 4,6- dimethyl DBT (4,6-DMDBT), pyrrole and quinoline), representatives of those contained in Diesel fuels. As well, model Diesel blends, added with these compounds, and were tested in order to emulate a real Diesel composition. Adsorption isotherms were determined at room temperature in the case of the pure compounds and were fitted to either Langmuir or Tempkin models. In all cases, TiO_2 nanotubes showed a higher adsorption performance, either at breakthrough or saturation capacity. For instance, at breakthrough adsorption, TiO_2 nanotubes adsorbed 230 and 41 times more DBT and 4,6-DMDBT, respectively, than those in TiO_2 nanoparticles. As well, at breakthrough point, TiO_2 nanotubes adsorbed 22 and 7.8 times more pyrrole and quinoline, respectively, than those in TiO_2 nanoparticles. Saturation adsorption capacity of TiO_2 nanotubes is 1.7-1.8 times higher for S-compounds and, 1.4-1.9 times higher for N-compounds than that of TiO_2 nanoparticles. In a model Diesel blend, selectively N-compounds were lowered considerably, 50 and 81% for quinoline and pyrrole, respectively, while S-compounds remained almost unchanged. These results confirm that TiO_2 nanotubes have a strong preference for N-compounds when exposed to Diesel blends having competing S-compounds.*

Keywords— Adsorption of organo-nitrogen, organo-sulphur, Sulphur, Titania Nanotube, adsorption properties, Liquid-phase.

I. INTRODUCTION

Air pollution has been a matter of great concern because of the serious environmental and health problems, which derived from it. An important air pollution source is the vehicle emissions produced during the combustion of fuels. In order to control these emissions, the governments of many countries have established strict regulations for the content of different compounds in transportation fuels. Particularly, sulphur levels are controlled to prevent deactivation of catalytic converter in gasoline vehicles; eventually SO_x emissions contribute to acid rain. In the US, the maximum allowable sulphur content in diesel is 15 ppmw (parts per million by weight) meanwhile in the EU is 10 ppmw [1-6]. In addition, interest in ultra-low sulphur fuels is motivated by the need of using new emission-control technology and fuel cells [2,7-10].

Oil Refineries traditionally employ hydrodesulphurization process (HDS) to remove organosulphur compounds from feedstocks for diesel production; but achieving ultra-low sulphur levels solely on this process has become a difficult task, because of the alkylsubstitued dibenzothiophenes (i.e. refractory sulphur) which are not easily eliminated [11,12]. Therefore, several alternatives have been applied to improve the efficiency of HDS: catalysts activity enhancement, increase of HDS process severity, use of complementary non-catalytic process, among others [9,13-16]. An additional challenge that must be solved is the removal of HDS catalysts inhibitors, specially nitrogen compounds which have comparable or lower reactivity than refractory sulphur species [9,17-20]. Basic and non-basic nitrogen molecules naturally occurring in oil feedstocks for fuel production are eliminated by hidrodenitrogenation (HDN); however, this process is significantly more difficult to carry out than HDS [11,21]. Both reactions occur simultaneously. so any reduction in nitrogen prior to the desulphurization will enhance efficiency of the later [22,23]. Denitrogenation process is also important to prevent NO_x emissions upon fuel combustion [21,24].

The removal of organosulphur and organonitrogen molecules is a key factor to produce clean fuels that current legislation demands but new or improved technologies are needed to reach this goal. Among these technologies are oxidation [25-30], extraction [31-35], alkylation [36-38], precipitation [39-43], biodesulphurization [44], biodenitrogenation [45,46] and adsorption [9,47].

Particularly, adsorption is an attractive approach since it does not require high temperature or high pressure and little or no hydrogen is needed. [9,48]. Several efforts have been made to understand different adsorption aspects like selectivity, adsorption capacity, regenerability, and adsorption mechanism. All these issues depend on the adsorbent material and the characteristics of the target feedstock. Therefore, diverse materials have been examined for this end in the adsorption of sulphur and nitrogen compounds contained in oil fractions. Hernandez-Maldonado et al. reported studies using zeolites with different metal cations including Ag^{+}, Cu^{+}, Ni^{2+} and Zn^{2+} [49-53]. These ion-exchanged materials rely on a mechanism called π-complexation to selectively remove organosulphur or organonitrogen molecules from commercial fuels. Also, Song and co-workers developed zeolite adsorbents for desulphurization but they suggested a mechanism based on a direct interaction between sulphur atom and the adsorption sites [9,54]. Activated carbon is another interesting material that has been tested in adsorption due to its high specific surface area, pore size distribution and surface properties which can be modified adding some functional groups [23,48,55-57]. Furthermore, other researchers proposed the use of single or combined metal oxides as an option for the production of sulphur and nitrogen adsorbents. Zinc oxide was reported as the main component of the adsorbent designed for S-Zorb process, although alumina, silica and nickel oxide are also part of it [59]. Several studies reported the use of alumina, single or mixed, in desulphurization and/or denitrogenation of gasoline and diesel [4,48,59,60]. Adsorption of organosulphur or organonitrogen compounds on anatase TiO_2 was neglected for many years, probably because the low surface area values typical of conventional anatase (< 100 m^2 /g), these numbers being even much lower when dealing with rutile TiO_2 (< 30 m^2/g). Nonetheless, the development of TiO_2 nanotubes resulted in materials having specific surface area of between 300-500 m^2/g, turning these materials more attractive from the adsorption and/or catalysis application viewpoint [61, 62, 63]. The greater the surface area exposed on a given adsorbent the lower the mass or volume necessary to fill an eventual separation reservoir, once in a final application. The adsorption of gaseous nitrogen and sulphur containing molecules on anatase and rutile TiO_2 surfaces were largely investigated to characterize the TiO_2 surface reactivity [64 and references therein]. In general, it was established that these molecules can be bonded to coordinatively unsaturated Ti sites or to fill the O-vacancies on oxygen deficient surfaces, however the total amount of adsorbed sulphur was affected by surface hydroxyl group coverage and molecularly adsorbed water layer [65]. Conversely, the adsorption of sulphur molecules bonded to complex organic conjugated rings, such as thiophene and its derivatives, on TiO_2 has been scarcely explored experimentally [66]. A $Ti_xCe_{1-x}O_2$ material was proposed as a promising adsorbent of sulphur molecules contained on liquid hydrocarbon fuels. Titania-based materials are encouraging as adsorbents for adsorptive desulphurization processes due to selective S−Ti binding and regenerability in oxygen/air flows. To understand the adsorption mechanism of thiophenic compounds on TiO_2-based adsorbents for ultra-deep desulphurization of liquid hydrocarbon fuels, theoretical studies of density functional theory (DFT) were conducted on the adsorption of thiophene on modeled anatase TiO_2 (0 0 1) surface [67,68,69]. Herein, we report for the first time the adsorption of sulphur and nitrogen compounds contained in light or intermediate petroleum fractions over nanostructured (nanotubes and nanofibers) TiO_2.

In the present work with a view to examine the influence of TiO_2 morphology, adsorptive desulphurization and denitrogenation of a model diesel fuel was carried out on TiO_2 nanotubes (titanate nanotubes) and compared with that of a commercial anatase. The equilibrium adsorption behavior was examined using the adsorption isotherm technique on liquid phase batch adsorption experiments. As well, dynamic flow adsorption in a fixed-bed system, at ambient temperature and atmospheric pressure using titanate nanotubes and a commercial anatase was carried out. The adsorptive capacity on different organosulphur and organonitrogen compounds at breakthrough and saturation point were evaluated.

II. EXPERIMENTAL

2.1 Adsorbents and model diesel fuels

Nanotubular titanate used as adsorbent was obtained by a hydrothermal method described in [61] starting from a commercial anatase (Hombikat K03 purchased from Sachtleben Chemie GmbH). Characterization of nanotubular titania were described in a previous work [61]. In order to establish the influence of TiO_2 nanoparticles transformation of into nanotubes, the commercial anatase was used as a reference adsorbent. The material had a crystallite size of 20 nm and specific surface area of 101 m^2/g.

Four different model diesel fuels (MDF) were prepared for batch adsorption experiments using sulphur or nitrogen compounds. The MD1 and MD2 model diesel fuels were prepared with dibenzothiophene (DBT, ≥99%) or 4,6-dibenzothiophene (4,6-DMDBT, 97%), dissolved in hexadecane (≥99%) containing 628 and 111 ppmw S, respectively. The MD3 and MD4 model fuels were prepared using pyrrole (98%) or quinoline (98%) dissolved in a toluene (99.9%)–hexadecane mixture 20% and 80 vol%, with a 447 and 117 ppmw N, respectively. All chemicals were from Sigma-Aldrich.

For fixed-bed adsorption experiments, four new model diesel fuels were prepared following the above procedure. The MD5 model diesel contained DBT with a final 730 ppmw S concentration, whereas MD6 fuel contained 4,6-DMDBT with 143 ppmw S. Model fuels containing nitrogen were prepared with pyrrole (MD7) and quinoline (MD8) whose final concentrations were 380 and 100 ppmw N, respectively. In order to determine the adsorption selectivity, a model diesel (MD9) containing all the above N and S components were prepared in a 20% toluene-80% hexadecane solvent, with DBT to a final 531 ppmw S; 4,6-DMDBT 220 ppmw S; pyrrole with 294 ppmw N; and quinoline 131 ppmw N.

2.2 Batch adsorption experiments

Liquid phase adsorptive desulphurization and denitrogenation in a batch system were measured at room temperature (20ºC) and atmospheric pressure. Different dosages of the TiO_2 adsorbent were added using constant volumes of the above described model fuels, then, the mixtures were shaken with magnetic stirrers in order to reach equilibrium (typically, 0.5 h). Subsequently, the supernatant liquid was extracted, passed through PTFE syringe filters and stored in vials. Sulphur and/or nitrogen concentration was analyzed to measure the adsorption capacity of the titanate nanotubes. The amount of S or N adsorbed at equilibrium, in milligrams per gram of solid, q_e, was calculated according to the following equation:

$$q_e = \frac{L(C_0 - C_e)}{m}$$

where L is the liquid fuel weight (kg), C_o and C_e are the initial and equilibrium concentrations of the solute in the liquid fuel (mg/kg), respectively, and m is the amount of adsorbent used (g).

2.3 Fixed bed adsorption experiments

Dynamic adsorption experiments were carried out using the system represented in Fig. 1. The adsorption processes were performed at room temperature and atmospheric pressure using titanate nanotubes or anatase nanoparticles as adsorbents and MD5-MD8 fuels. A glass column of 3 cm i.d. and 33 cm length was packed with 2 g of adsorbent (80-100 mesh) and placed in a furnace designed for this purpose. Prior to adsorption, materials were heated at 300ºC for 3 h in nitrogen (flow rate: 200 cm^3/min). After this pretreatment, the adsorbent was allowed to cool to room temperature and then hexadecane was introduced into the inlet of the column using a peristaltic pump at 1 cm^3/min in order to remove any entrapped gas. Then, the hexadecane head was allowed to dissipate and the feed was exposed to the model diesel with S or N compounds, using the same flow rate as that of the hydrocarbon. Effluent samples were collected periodically until saturation of the adsorbent.

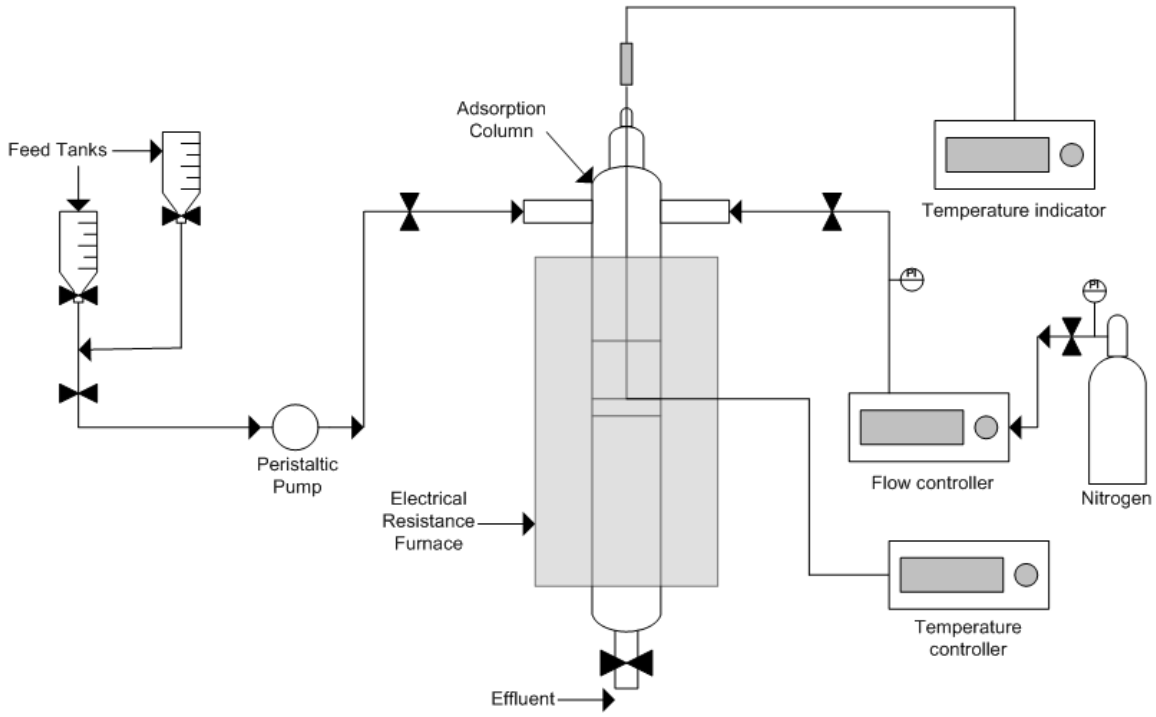

FIG. 1. EXPERIMENTAL SYSTEM USED FOR DYNAMIC ADSORPTION PROCESSES

Breakthrough and saturation adsorption capacities were calculated using the following equation:

$$q_{breakthrough\ or\ saturation} = \left(\frac{\dot{v}}{m_{adsorbent}} \right) \left(\rho_{fuel}\, X_i \right) \int_0^t \left[1 - \frac{C}{C_0} \right] dt$$

where q is the total adsorbed S or N (mg S or N/g adsorbent), $\dot{v}$ is the flow rate of the feed (mL/min), $m_{adsorbent}$ is the weight of the adsorbent bed (g), ρ_{fuel} is the fuel density (g/mL) at room temperature, X_i is the total S or N fraction (by weight) in the feed, C_0 is the initial S or N concentration in the feed (ppmw), C is the S or N effluent concentration (ppmw) at time t (min).

2.4 Sulphur and nitrogen analysis

S or N concentrations in all collected samples were measured using an Antek 9000 total S or N analyzer, except for S concentration in effluent samples obtained in dynamic adsorption, for which, an energy dispersive X-ray fluorescence (EDXRF) spectrometer, model S2 Ranger supplied by Bruker was employed.

III. RESULTS AND DISCUSSION

3.1 Adsorption isotherms

Batch mode experiments were conducted in order to explore adsorption performance of titanate nanotubes in adsorptive desulphurization and denitrogenation of model diesel fuels (MD1-MD4). Experimental data were used to construct the equilibrium isotherms for each organosulphur and organonitrogen compound. The sulphur adsorption capacities, q_e, as a function of the equilibrium concentrations, C_e, in the liquid phase appear in Figure 2.

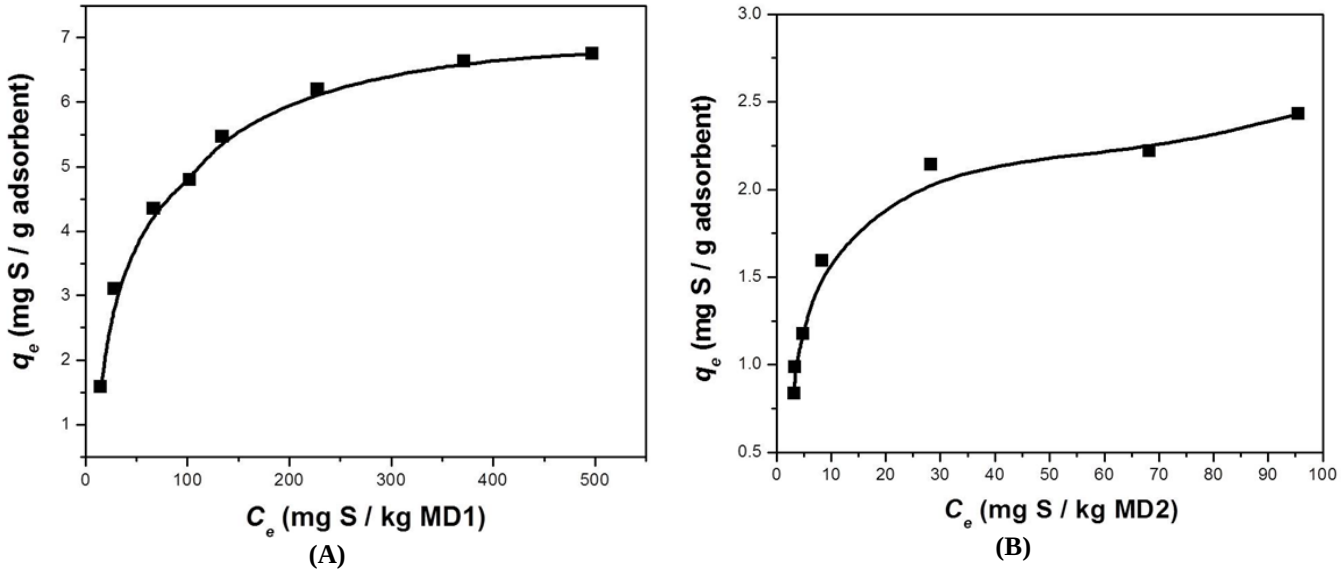

FIG. 2. EQUILIBRIUM ADSORPTION ISOTHERMS OF (A) DBT AND (B) 4,6-DMDBT OVER TITANATE NANOTUBES.

The isotherm shape indicates a favorable adsorption of the corresponding adsorbate (DBT or 4,6-DMDBT) [70]. It can be observed in the plots (Fig. 2 (A) and (B)) that the adsorption capacity raises gradually as the equilibrium concentration of the adsorbate in the liquid phase increased. In both cases, the highest added adsorbent amount belongs to the first point of the isotherm meanwhile the last point represents the minor amount of it. In these experiments, the fuel volume remained constant while the varying parameter was the adsorbent dosage; therefore, the observed q_e increase with the decrease of the adsorbent amount can be explained on the basis of adsorption sites density. As reported in an earlier work, the main adsorption sites on titania nanotubes surface were OH groups [61,71], then, when the number of these sites decrease while keeping a constant adsorbate concentration, there will be more adsorbed molecules per adsorption site resulting in higher q_e values.

The same behavior was observed for adsorption isotherms of nitrogen compounds whose shape also indicated a favorable adsorption. In Fig. 3 (A) the nitrogen adsorption capacity, q_e, increases gradually as the equilibrium concentration of pyrrole in treated model fuel, C_e, rose. On the other hand, the first part of the quinoline adsorption isotherm (Fig. 3 (B)) shows an increase in adsorption capacity meanwhile the equilibrium concentration remained near zero indicating almost complete adsorption of this nitrogen molecule. In addition, the highest and lowest dosages of titania nanotubes belong to the first and

last point of the isotherm, respectively. Then, the q_e increase with the decrease of adsorbent dosage could also be related to adsorption sites density. It is worth mentioning that the initial toluene percentage, which is an aromatic component in model diesel, remained almost at the same value after adsorption, suggesting a negligible interaction with adsorption sites on titanate nanotubes. This fact also indicates a non-competitive adsorption between aromatic compounds and nitrogen molecules.

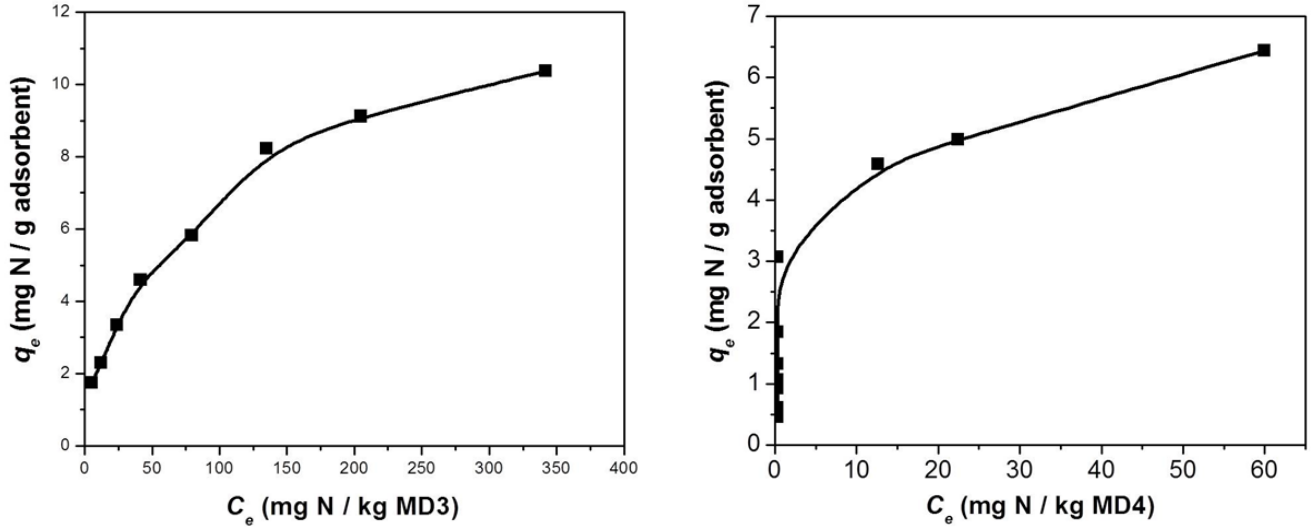

FIG. 3. EQUILIBRIUM ADSORPTION ISOTHERMS OF (A) PYRROLE AND (B) QUINOLINE OVER TITANATE NANOTUBES.

To approximate the behavior of the different adsorbates on the titanate nanotubes surface three-adsorption isotherm equations were applied: Langmuir, Freundlich and Temkin. The equation constants and the determination coefficients (R^2) are listed in Tables 1, 2 and 3 respectively. According to R^2 values, Langmuir and Temkin models gave better fit to the DBT adsorption isotherm, while for 4,6-DMDBT the best fit was only for the former model. Comparing the Langmuir isotherm parameters of the two sulphur compounds, it can be noted that *Q* (capacity of the monolayer) is higher for DBT, indicating a superior adsorption capacity of the titanate nanotubes with respect to this molecule [70,72,73]. However, *b* (adsorption equilibrium constant) had a higher value for 4,6-DMDBT, then, a stronger interaction between this molecule and nanotubes adsorption sites (OH groups) occurred [70,72,73].

TABLE 1
LANGMUIR ISOTHERM PARAMETERS FOR THE REMOVAL OF SULPHUR AND NITROGEN COMPOUNDS BY TITANIA NANOTUBES.

Langmuir	$q_e = \frac{QbC_e}{1+bC_e}$		
	Q(mg / g)	***b (1/ppmw)***	R^2
DBT	7.94	0.01	0.9772
4,6-DMDBT	2.52	0.17	0.9746
Pyrrole	7.28	0.05	0.9029
Quinoline	5.45	1.08	0.8499

TABLE 2
FREUNDLICH ISOTHERM PARAMETERS FOR THE REMOVAL OF SULPHUR AND NITROGEN COMPOUNDS BY TITANIA NANOTUBES

Freundlich	$q_e = K_F C_e^{1/n}$		
	$K_F(mg^{1-1/n}\ kg^{1/n}/g)$	*1/n*	R^2
DBT	0.748	0.382	0.8904
4,6-DMDBT	0.717	0.284	0.9041
Pyrrole	0.798	0.454	0.9901
Quinoline	1.979	0.299	0.9441

For pyrrole adsorption, the Freundlich model had the highest R^2 value, Table 3, reflecting heterogeneous adsorption due to energetically different adsorption sites [70,73]. The parameter K_F represents the adsorption capacity while *1/n* is indicative of adsorption intensity. Values of $1/n < 1$ stand for favorable adsorption conditions [70,72,73]. Additionally, the equilibrium adsorption data for quinoline are better described by Temkin equation in which A and *B* are constants. The value of B parameter denotes favorable adsorption; this fact is in accordance with the isotherm shape observed on other adsorbents [73].

TABLE 3
TEMKIN ISOTHERM PARAMETERS FOR THE REMOVAL OF SULPHUR AND NITROGEN COMPOUNDS BY TITANIA NANOTUBES

Temkin	$q_e = A\ln(BC_e)$		
	A	*B (kg/g)*	R^2
DBT	1.48	0.25	0.9788
4,6-DMDBT	0.44	2.89	0.9548
Pyrrole	2.20	0.25	0.9532
Quinoline	0.89	15.49	0.9798

3.2 Breakthrough curves

In a comparison of the dynamic adsorption process, the two adsorbents, titanate nanotubes and commercial anatase nanoparticles (Hombikat K03), were tested in the removal of sulphur and nitrogen compounds from model diesels (MD5-MD8) blends, using a fixed-bed system at ambient temperature and atmospheric pressure. The adsorption capacity for the different organosulphur and organonitrogen compounds at breakthrough and saturation point were evaluated on the basis of breakthrough curves which were generated by plotting the effluent transient sulphur or nitrogen concentration, *C*, normalized by the feed, C_0, versus cumulative effluent fuel volume normalized by total bed weight.

TABLE 4
BREAKTHROUGH AND SATURATION ADSORPTION CAPACITIES FOR ANATASE NANOPARTICLES AND TITANATE NANOTUBES

Adsorbate	$q_{breakthrough}$ (mg S or N / g adsorbent)		$q_{saturation}$ (mg S or N / g adsorbent)	
	Anatase Hombikat K03	Titanate nanotubes	Anatase Hombikat K03	Titanate nanotubes
DBT	0.02	4.6	9.2	16.5
4,6-DMDBT	0.08	3.3	4.5	7.7
Pyrrole	0.10	2.2	14.4	20.8
Quinoline	0.58	4.5	5.7	10.7

MD5 was treated with anatase and titanate nanotubes, respectively, their breakthrough curves are shown in Fig. 4 (A). It can be seen that the anatase breakthrough curve exhibited high C/C_0 values at an early stage indicating an important sulphur amount in the effluent. This performance implied a low adsorption capacity of anatase nanoparticles and also suggests a lack of strong interactions between the adsorbent and adsorbate. A different behavior was observed for titanate nanotubes breakthrough curve in which the relation C/C_0 increased gradually at higher amounts of treated fuel, reflecting a larger adsorption capacity than that of anatase. In these experiments the breakthrough point was fixed at an effluent sulphur concentration of 10 ppmw and saturation obviously was reached when the C/C_0 value equals 1.0. The calculated breakthrough and saturation sulphur adsorption capacities are listed in Table 4. The obtained results clearly show that titanate nanotubes had a much better performance than anatase nanoparticles in the adsorption of DBT sulphur at both breakthrough and saturation points. The difference observed in adsorption capacity may be related to specific surface area, morphology and surface chemical properties. First, titanate nanotubes had higher specific surface area (320 m^2/g) [61] than anatase nanoparticles (101 m^2/g), second the morphology greatly influence the accessibility and the surface chemistry of materials. According to previous studies, surface adsorption sites on TiO_2 materials changed with morphology [71]; the studies demonstrated that nanotubular titania has mainly OH groups on its surface while anatase nanoparticles is characterized by surface Ti^{4+} cations [71]. Also, nanotubes used in this work had only OH groups at their surface as reported in a previous work [61]. On the basis of these different results, the higher adsorption capacity found in titanate nanotubes suggests that DBT had a stronger interaction with OH groups than with Ti^{4+}. Furthermore, said interaction might be via the formation of

H-bonds between the proton of OH groups and S atom in DBT molecule, since non-Brönsted nature prevails in OH groups [71].

The model diesel fuel prepared with 4,6-DMDBT (MD6) was also treated with titanate nanotubes and anatase nanoparticles. The breakthrough curves for 4,6-DMDBT sulphur adsorption are shown in Fig. 4 (B). With anatase nanoparticles breakthrough curve rapidly reached C/C_0 values over 0.08 and saturation was clear at a very early stage; the breakthrough point fixed at 10 ppmw S was exceeded from the beginning. Breakthrough curve behavior indicated a low 4,6-DMDBT sulphur adsorption capacity and also suggests the existence of very weak interactions between adsorbent and adsorbate. On the other hand, titanate nanotubes breakthrough curve showed a slow C/C_0 increase at larger volumes of treated fuel up to saturation, reflecting a superior sulphur adsorption capacity. Table 4 shows the breakthrough and saturation sulphur adsorption capacities which validate a better performance of titanate nanotubes in the adsorption of 4,6-DMDBT. As in the case of DBT, the higher adsorption capacity of nanotubes could be related to their specific surface area, morphology and nature of surface sites. Aside from having different surface adsorption sites on titanate nanotubes and anatase nanoparticles, the accessibility to these sites could play an important role in the adsorption of 4,6-DMDBT. As reported elsewhere by our group [71], nanotubular titania have more accessible adsorption sites (OH groups), therefore, a stronger interaction can be expected between 4,6-DMDBT and protons exposed on the curved nanotubular surface than with adsorption sites (Ti^{4+} cations) located at nanoparticles flat surface. The steric hindrance conferred by the two methyl groups located in 4 and 6 positions of 4,6-DMDBT reduces the interaction with a protruding proton on a curved nanotubular structure.

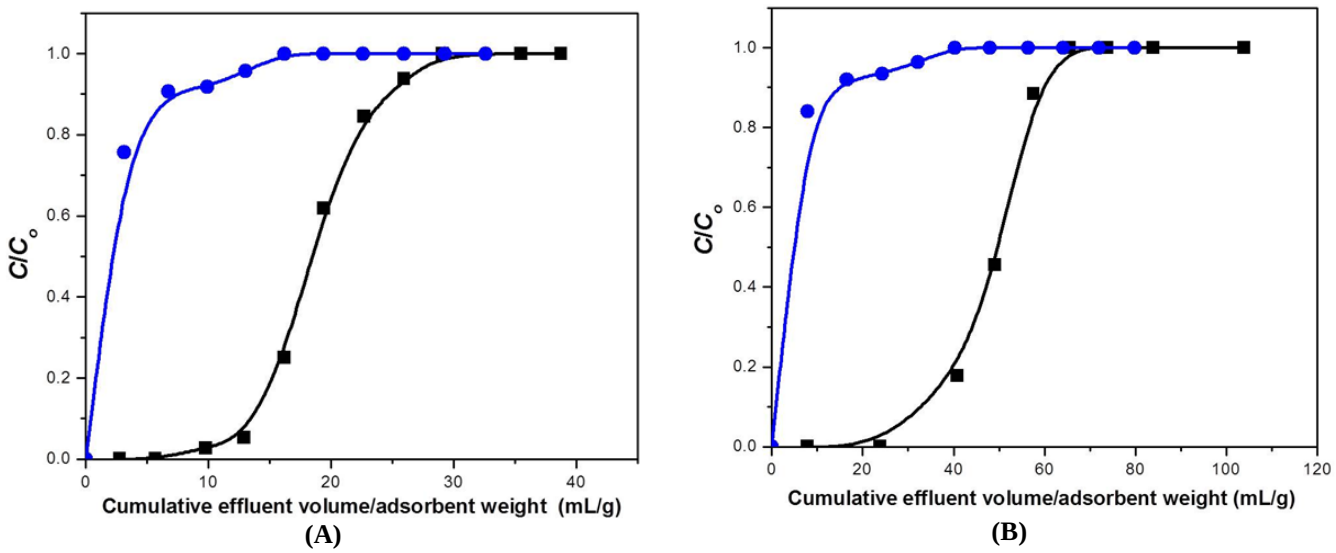

FIG. 4. BREAKTHROUGH CURVES OF (A) DBT AND (B) 4,6-DMDBT OVER (■)TITANATE NANOTUBES AND (●)ANATASE NANOPARTICLES.

In a comparison of DBT and 4,6-DMDBT sulphur adsorption capacity on nanotubes, the lower value obtained for the latter compound suggests that steric hindrance might play an important role in adsorption process, although it was reduced to certain extent, due to the accessibility of OH groups located on the curved nanotubular surface. This result also suggests a direct interaction between S atom of the model organosulphur compounds and the proton of OH groups that may occur via the formation of H-bonds.

The literature on adsorptive desulphurization reported the performance of various adsorbents using model and commercial diesel. For instance, Song et al. desulphurized model diesel using activated carbon derived from coconut and wood, obtained breakthrough and saturation adsorption capacities of approximately 6.5 and 16.7 mg S/g adsorbent, respectively for the former and 4.3 and 13.1 mg S/g adsorbent for the latter [3]. Also, Mochida et al. removed sulphur using activated carbon from a hydrotreated gasoil for which the breakthrough adsorption capacity was reported to be approximately 10 mg S/g adsorbent [74]. On the other hand, also a successful group of adsorbents was developed by Hernández-Maldonado and co-workers. They synthesized ion exchanged zeolites to remove not only sulphur but nitrogen compounds from commercial diesel; the highest total sulphur adsorption capacity reported was approximately 8.89 and 13.12 mg S/g adsorbent at breakthrough and saturation, respectively, for Cu(I)-Y zeolite [49,50]. Lower total sulphur adsorption capacities were reported for other ion-exchanged zeolites: Cu(I)-Y 5.34 and 11.96 mg S/g adsorbent, Ni(II)-X 4.57 and 8.03 mg S/g adsorbent, Ni(II)-Y 5.05 and 9.24 mg S/g adsorbent, Ce(IV)-Y 1.37 and 3.90 mg S/g adsorbent, the former values belong to

the breakthrough and the latter to saturation [50,75]. Furthermore, Hernández-Maldonado et al. increased the sulphur removal making use of guard beds of activated carbon and/ or alumina in combination with zeolite adsorbents [51,76]. However, they observed that the amount of aromatics played an important role in diminishing the sulphur removal capacity [76]. The values of sulphur adsorption capacity reported for titanate nanotubes in this study are in the range of that obtained for some ion-exchanged zeolites, although, the model fuel only contained DBT or 4,6-DMDBT as sulphur compounds. This fact indicates that titanate nanotubes may be a promising adsorbent for desulphurization of fuels.

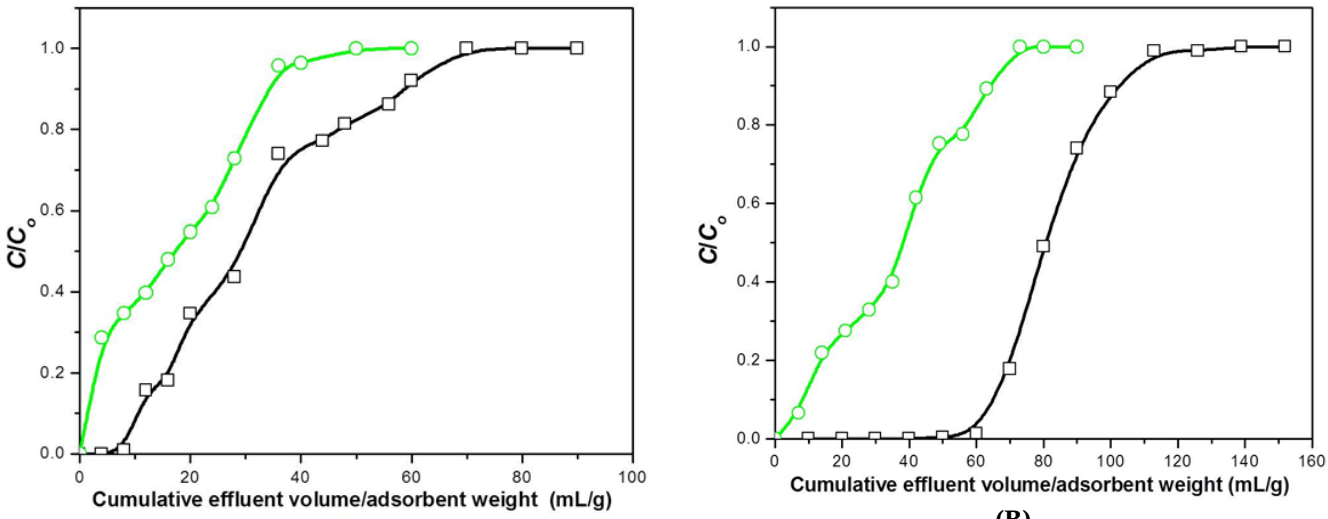

FIG. 5. BREAKTHROUGH CURVES OF (A) PYRROLE AND (B) QUINOLINE OVER (□)TITANATE NANOTUBES AND (○)ANATASE NANOPARTICLES.

Additionally, our adsorbents were tested in denitrogenation of MD7 and MD8 which contained pyrrole or quinoline, respectively. The breakthrough curves for the adsorption of pyrrole over anatase and nanotubes are shown in Fig. 5 (A). It can be observed that for anatase nanoparticles the C/C_0 values increased gradually, indicating a moderate adsorption of pyrrole molecules; however the breakthrough point fixed in 10 ppmw N was overtaken from the begging of the process. A better adsorption performance was seen for nanotubes breakthrough curve in which C/C_0 values also increased gradually but at higher volumes of treated fuel. The calculated breakthrough and saturation adsorption capacities are listed in Table 4 in which nanotubes have larger values as expected from the behavior of breakthrough curves. It is worth mentioning that the percentage of toluene in untreated model fuel remained almost the same after adsorption process, indicating a minor adsorption of this aromatic compound, if any, in both anatase and nanotubes. This result agrees with that obtained in batch adsorption.

As mentioned above, in the adsorption of organosulphur molecules a better performance of nanotubes in the adsorption of pyrrole can be attributed to physicochemical characteristics. The larger value of nanotubes specific surface area, morphology, the type and the accessibility of adsorption sites might contribute to enhance adsorption. The obtained results also suggest a stronger interaction between OH groups in nanotubes and pyrrole molecules than with anatase´s Ti^{4+} cations.

Finally, the breakthrough curves in the adsorption of quinoline over anatase and titanate nanotubes are presented in Fig. 5 (B), in which a superior performance of nanotubes can be observed. In anatase breakthrough curve the C/C_0 values increased progressively reflecting a moderate quinoline adsorption up to saturation. The adsorption of quinoline over anatase might be due to an acid-base interaction between the lone electron pair located in nitrogen atom and Ti^{4+} cations that exist at the surface of the adsorbent, since in our previous work, said interaction was clearly revealed on pyridine and lutidine adsorption over anatase nanoparticles [71]. On the other hand, it is clear that a larger capacity for nitrogen adsorption can be obtained on titanate nanotubes, in view of the fact that around 65 mL of fuel with a N concentration lower than 10 ppmw were produced as showed by breakthrough curve. After breakthrough point, fixed at 10 ppmw, the C/C_0 value increased gradually reaching saturation at a treated fuel amount of 112 mL. The breakthrough and saturation adsorption capacities for both adsorbents are indicated in Table 4; which confirmed the superior performance of titanate nanotubes. Also, in these experiments the initial toluene percentage contained in model fuel remained almost at the same value after adsorption. The better performance of nanotubes in quinoline nitrogen adsorption again can be related to their specific surface area, morphology and type of adsorption sites (OH groups). According to pyridine and lutidine adsorption on titania nanotubes

reported previously by our group [71], the main interaction between these adsorbates and adsorbent was via H-bonding, therefore, it is expected that the same interaction had occurred between the lone electron pair located in N atom of quinoline and OH groups which are titanate nanotubes adsorption sites.

Comparing the pyrrole and quinoline nitrogen adsorption capacity of nanotubes a larger value was obtained at breakthrough point for the latter compound meanwhile at saturation the higher value was for the former. This behavior reflects a higher affinity for quinoline than for pyrrole.

Fewer results for denitrogenation of model and commercial diesel can be found in literature than for desulphurization ones. Mochida et al. studied adsorptive performance of activated carbon fibers in denitrogenation of a gasoil and the obtained capacity was 5.5 mg N/g adsorbent [74]. As well, Hernández-Maldonado et al. reported the use of Cu(I)-Y zeolite adsorbent combined with an activated carbon guard bed in denitrogenation of a commercial diesel for which an adsorption capacity at breakthrough point of approximately 3 mg N/g adsorbent was obtained [53]. Titanate nanotubes tested in this study presented a similar and superior adsorption capacity for nitrogen compounds according to the values reported in Table 4, furthermore, a minor adsorption of aromatic toluene was observed during denitrogenation, indicating a negligible competitive effect, if any, for adsorption sites of titanate nanotubes between heteronitrogen molecules and aromatics.

In order to establish the selectivity of adsorbent towards nitrogen or sulphur compounds, a model diesel, MD9, containing both nitrogen and both sulphur compounds were prepared and contacted with the titanates nanotubes at weight/volume ratio of 0.05. As can be seen in Table 5, nitrogen compounds were selectively adsorbed on the nanotubes. Around 81 and 50 % of pyrrole and quinoline respectively were eliminated from MD9 model diesel, whereas both sulphur compounds practically remained unchanged after adsorption process aiming that TiO_2 nanotubes absorb preferentially nitrogen compounds.

TABLE 5.
ADSORPTION SELECTIVITY OF TITANATE NANOTUBES ON N OR S ORGANO-COMPOUNDS CONTAINED IN A MODEL DIESEL

Adsorbate	MD9 (ppmw)	MD9 after adsorption (ppmw)	Amount of N or S adsorbed (%)
DBT	531	525	1.0
4,6-DMDBT	220	220	0
Pyrrole	294	56	81
Quinoline	131	65	50

IV. CONCLUSIONS

Titanate nanotubes are a promising adsorbent of organosulphur and organonitrogen compounds contained in diesel fuel, according to our results obtained in equilibrium and dynamic adsorption tests. Equilibrium adsorption experiments revealed favorable adsorption of sulphur (DBT, 4,6-DMDBT) and nitrogen (pyrrole, quinoline) molecules. The DBT adsorption experimental data fitted to a Langmuir and Temkin models, while for 4,6-DMDBT the Langmuir model had the best fit. Calculated parameters of Langmuir isotherm indicated that titanate nanotubes adsorbed higher higher amounts of DBT, however 4,6-DMDBT had a stronger interaction with them. In the case of nitrogen compounds, the Freundlich model fit better the pyrrole adsorption isotherm, reflecting heterogeneous adsorption due to energetically different adsorption sites meanwhile Temkin model better describe quinoline equilibrium adsorption data which takes into account some indirect interactions between adsorbate and adsorbent.

In fixed-bed adsorption experiments, titanate nanotubes had a much better performance than anatase nanoparticles in the adsorption of sulphur and nitrogen compounds. The difference observed in adsorption capacity may be related to specific surface area, morphology and/or surface chemical properties, such as surface functional group type. Also, the accessibility of the adsorption sites might play an important role especially in the adsorption of molecules with steric hindrance as in 4,6-DMDBT adsorption capacity values for anatase nanoparticles and titanate nanotubes. Particularly, the results of sulphur compounds adsorption on titanate nanotubes suggest the existence of a direct interaction between the heteroatom of the adsorbate and the surface OH groups in the adsorbent.

Results of fixed-bed nitrogen adsorption pointed out nanotubes have higher affinity for quinoline than for pyrrole, since at breakthrough point the adsorption capacity was higher for the former compound. According to previously reported

experiments [71], which suggest that the main interaction between quinoline and OH groups on titanate nanotubes occurred via H-bonding.

In addition, a negligible uptake of toluene on titanate nanotubes was observed in equilibrium and dynamic adsorption experiments. This fact represents an advantage of the nanotubes in desulphurization and denitrogenation of diesel fuels, which contain high amounts of aromatic compounds.

ACKNOWLEDGEMENTS

Adriana Rendón Rivera is indebted to CONACYT for a graduate student scholarship. The authors acknowledge financial support from Instituto Mexicano del Petróleo (Projects D.00246 and D.00483).

REFERENCES

[1] K.G. Knudsen, B.H. Cooper, H. Topsøe, Appl. Catal. A: Gen. 189 (1999) 205-215.
[2] X. Ma, L. Sun, C. Song, Catal. Today 77 (2002) 107-116.
[3] A. Zhou, X. Ma, C. Song, J. Phys. Chem. B 110 (2006) 4699-4707.
[4] J. Hyung Kim, X. Ma, A. Zhou, C. Song, Catal. Today 111 (2006) 74-83.
[5] J.M. Kwon, J.H. Moon, Y.S. Bae, D.G. Lee, H.C. Sohn, C.H. Lee, ChemSusChem 1 (2008) 307-309.
[6] M. Muzic, K. Sertic-Bionda, Z. Gomzi, S. Podolski, S. Telen, Chem. Eng. Res. Des. 88 (2010) 487-495.
[7] X. Ma, M. Sprague, C. Song, Ind. Eng. Chem. Res. 44 (2005) 5768-5775.
[8] Z. Cheng, X. Liu, J. Lu, M. Luo, React. Kinet. Catal. Lett. 97 (2009) 1-6.
[9] C. Song, Catal. Today 86 (2003) 211-263.
[10] C. Shalaby, X. Ma, A. Zhou, C. Song, Energy Fuels 23 (2009) 2620-2627.
[11] B.C. Gates, H. Topsøe, Polyhedron 16 (1997) 3213-3217.
[12] H. Rang, J. Kann, V. Oja, Oil Shale 23 (2006) 164-176.
[13] M. Breysse, G. Djega-Mariadassou, S. Pessayre, C. Geantet, M. Vrinat, G. Pérot, M. Lemaire, Catal. Today 84 (2003) 129-138.
[14] M.F. Ali, A. Al-Malki, S. Ahmed, Fuel Process. Technol. 90 (2009) 536-544.
[15] R. Shafi, G.J. Hutchings, Catal. Today 59 (2000) 423-442.
[16] F. van Looij, P. van der Laan, W.H.J. Stork, D. J. DiCamillo, J. Swain, Appl. Catal., A 170 (1998) 1-12.
[17] H. Schulz, W. Böhringer, P. Waller, F. Ousmanov, Catal. Today 49 (1999) 87-97.
[18] G.C. Laredo S., J.A. De los Reyes H., J.L. Cano D., J. Castillo M., Appl. Catal., A 207 (2001) 103-112.
[19] K.H. Choi, Y. Korai, I. Mochida, J.W. Ryu, W. Min, Appl. Catal., B 50 (2004) 9-16.
[20] P. Zeuthen, K.G. Knudsen, D.D. Whitehurst, Catal. Today 65 (2001) 307-314.
[21] P. Wiwel, K. Knudsen, P. Zeuthen, D. Whitehurst, Ind. Eng. Chem. Res. 39 (2000) 533-540.
[22] H. Yang, J. Chen, Y. Briker, R. Szynkarczuk, Z. Ring, Catal. Today 109 (2005) 16-23.
[23] Y. Sano, K.H. Choi, Y. Korai, I. Mochida, Energy Fuels 18 (2004) 644-651.
[24] H. Zhang, G. Li, Y. Jia, H. Liu, J. Chem. Eng. Data 55 (2010) 173-177.
[25] J.M. Campos-Martin, M.C. Capel-Sanchez, J.L. G. Fierro, Green Chem. 6 (2004) 557-562.
[26] J. Zhang, W. Zhu, H. Li, W. Jiang, Y. Jiang, W. Huang, Y. Yan, Green Chem. 11 (2009) 1801-1807.
[27] W. Zhu, H. Li, X. Jiang, Y. Yan, J. Lu, J. Xia, Energy Fuels 21 (2007) 2514-2516.
[28] G. Yu, S. Lu, H. Chen, Z. Zhu, Energy Fuels 19 (2005) 447-452.
[29] Y. Shiraishi, K. Tachibana, T. Hirai, I. Komasawa, Ind. Eng. Chem. Res. 41 (2002) 4362-4375.
[30] P. Q. Yuan, Z. M. Cheng, X.Y. Zhang, W.K. Yuan, Fuel 85 (2006) 367-373.
[31] S. Kumar, J. Gentry, Hydrocarbon Engineering 8 (2003) 27-28.
[32] J. Qi, Y. Yan, W. Fei, Y. Su, Y. Dai, Fuel 77 (1998) 255-258.
[33] S. Zhang, Q. Zhang, Z.C. Zhang, Ind. Eng. Chem. Res. 43 (2004) 614-622.
[34] H. Li, W. Zhu, Y. Wang, J. Zhang, J. Lu, Y. Yan, Green Chem. 11 (2009) 810-815.
[35] E.S. Huh, A. Zazybin, J. Palgunadi, S. Ahn, J. Hong, H.S. Kim, M. Cheong, B. S. Ahn, Energy Fuels 23 (2009) 3032-3038.
[36] B.D. Alexander, G.A. Huff, V. R. Pradhan, W.J. Reagan, R.H. Cayton US Patent 6,024,865 (2000).
[37] N.A. Collins, J.C. Trewella US Patent 5,599,441 (1997).
[38] B.H. Olivier, D. Uzio, F. Diehl, M. Lionel FR Patent 2,840,916 (A1) (2003).
[39] V. Meille, E. Schulz, M. Vrinat, M. Lemaire, Chem. Commun. (1998) 305-306.
[40] A. Milenkovic, E. Schulz, V. Meille, D. Loffreda, M. Forissier, M. Vrinat, P. Sautet, M. Lemaire, Energy Fuels 13 (1999) 881-887.
[41] Y. Shiraishi, Y. Taki, T. Hirai, I. Komasawa, Ind. Eng. Chem. Res. 40 (2001) 1213-1224.

[42] Y. Shiraishi, K. Tachibana, T. Hirai, I. Komasawa, Ind. Eng. Chem. Res. 40 (2001) 3390-3397.
[43] Y. Shiraishi, K. Tachibana, T. Hirai, I. Komasawa, Ind. Eng. Chem. Res. 40 (2001) 4919-4924.
[44] S.C.C. Santos, D.S. Alviano, C.S. Alviano, M. Pádula, A.C. Leitão, O.B. Martins, C.M. Ribeiro, M.Y.M. Sassaki, C.P.S. Matta, J. Bevilaqua, G.V. Sebastián, L. Seldin, Appl. Microbiol. Biotechnol. 71 (2006) 355-362.
[45] M.J. Benedik, P.R. Gibbs, R.R. Riddle, R.C. Willson, Trends Biotechnol. 16 (1998) 390-395.
[46] S. Le Borgne, R. Quintero, Fuel Process. Technol. 81 (2003) 155-169.
[47] A.J. Hernández-Maldonado, R. T. Yang, Catal. Rev.: Sci. Eng. 46 (2004) 111-150.
[48] M. Almarri, X. Ma, C. Song, Ind. Eng. Chem. Res. 48 (2009) 951-960.
[49] A.J. Hernández-Maldonado, R. T. Yang, J. Am. Chem. Soc. 126 (2004) 992-993.
[50] A.J. Hernández-Maldonado, F. H. Yang, G. Qi, R. T. Yang, Appl. Catal., B 56 (2005) 111-126.
[51] A.J. Hernández-Maldonado, S.D. Stamatis, R.T. Yang, A.Z. He, W. Cannella, Ind. Eng. Chem. Res. 43 (2004) 769-776
[52] R.T. Yang, A. Takahashi, F.H. Yang, Ind. Eng. Chem. Res. 40 (2001) 6236-6239.
[53] A.J. Hernández-Maldonado, R.T. Yang, Angew. Chem. Int. Ed. 43 (2004) 1004-1006.
[54] X. Ma, S. Velu, J. Hyung Kim, C. Song, Appl. Catal., B 56 (2005) 137-147.
[55] Y. Sano, K. H. Choi, Y. Korai, I. Mochida, Appl. Catal., B 49 (2004) 219-225.
[56] A. Zhou, X. Ma, C. Song, J. Phys. Chem. B 110 (2006) 4699-4707.
[57] A. Zhou, X. Ma, C. Song, Appl. Catal., B 87 (2009) 190-199.
[58] I.V. Babich, J.A. Moulijn, Fuel 82 (2003) 607-631.
[59] J. Wu, X. Li, W. Du, C. Dong, L. Li, J. Mater. Chem. 17 (2007) 2233-2240.
[60] A. Srivastav, V.C. Srivastava, J. Hazard. Mater. 170 (2009) 1133-1140.
[61] A. Rendón-Rivera, J.A. Toledo-Antonio, M.A. Cortés-Jácome, C. Angeles-Chávez, Catal. Today 166 (2011) 18-24.
[62] J.A. Toledo-Antonio, S. Capula, M.A. Cortes-Jacome, C. Angeles-Chavez, E. Lopez-Salinas, G. Ferrat, J. Navarrete, J. Escobar, J. Phys. Chem. C 111 (2007) 10799-10805.
[63] T. Kasuga, M. Hiramatsu, A. Hoson, T. Sekino, K. Niihara, Langmuir 14 (1998) 3160-3163.
[64] U. Diebold, Surf. Sci. Rep. 48 (2003) 53-229
[65] J. Baltrusaitis, P.M. Jayaweera, V.H. Grassian, J. Phys. Chem. C 115 (2011) 492–500
[66] S. Watanabe, X. Ma, C. Song, Prepr. Pap. –Am. Chem. Soc., Div. Fuel Chem. 49 (2) (2004) 511-513.
[67] S. Sitamraju, M.J. Janik, C. Song, Top Catal 55 (2012) 229–242.
[68] J. Guo, M. J. Janik, C. Song, J. Phys. Chem. C 116 (2012) 3457−3466.
[69] J. Guo, S. Watanabe, M.J. Janik, X. Ma, C. Song, Catal. Today 149 (2010) 218–223.
[70] F.L. Slejko, Adsorption technology: a step by step approach to process evaluation and application, Marcel Dekker, New York, 1985.
[71] J.A. Toledo-Antonio, M.A. Cortés-Jácome, J. Navarrete, C. Angeles-Chávez, E. López-Salinas, A. Rendón-Rivera, Catal. Today 155 (2010) 247-254.
[72] J.D. Seader, E.J. Henley, Separation Process Principles, John Wiley & Sons, United States of America, 1998.
[73] B.H. Hameed, D.K. Mahnoud, A.L. Ahmad, J. Hazard. Mater. 185 (2008) 65-72.
[74] Y. Sano, K. Sugahara, K.H. Choi, Y. Korai, I. Mochida, Fuel 84 (2005) 903-910.
[75] A.J. Hernández-Maldonado, R. T. Yang, Ind. Eng. Chem. Res. 43 (2004) 1081-1089.
[76] A.J. Hernández-Maldonado, R. T. Yang, Ind. Eng. Chem. Res. 42 (2003) 3103-3110.